chemistry proceedings

MDPI

Proceeding Paper

In Silico Study of Obeticholic Acid Analogs as FXR Agonists †

Julio A. Seijas [1,*], Silvia Vázquez-Gómez [2], Francisco Meijide [3] and M. Pilar Vázquez-Tato [1]

[1] Departamento de Química Orgánica, Facultade de Ciencias, Universidade de Santiago de Compostela, Campus Terra, 27080 Lugo, Spain; pilar.vazquez.tato@usc.es
[2] Hospital Álvaro Cunqueiro, 36312 Vigo, Pontevedra, Spain; silvia.vazquez.gomez@sergas.es
[3] Departamento de Química Física, Facultade de Ciencias, Universidade de Santiago de Compostela, Campus Terra, 27080 Lugo, Spain; francisco.meijide@usc.es
* Correspondence: julioa.seijas@usc.es
† Presented at the 29th International Electronic Conference on Synthetic Organic Chemistry (ECSOC-29); Available online: https://sciforum.net/event/ecsoc-29.

Abstract

Nuclear receptors are ligand-activated transcription factors that, in response to lipophilic hormones, vitamins, and dietary lipids, regulate numerous aspects of mammalian physiology. Bile acid receptors represent well-defined targets for the development of novel therapeutic approaches for metabolic and inflammatory diseases. The farnesoid X receptor (FXR) was identified as an orphan steroid receptor-like nuclear receptor, and its activation is crucial in many physiological functions of the liver. A vital function of FXR is to influence the amount of bile acids in hepatocytes by reducing bile acid synthesis, stimulating the bile salt export pump, and inhibiting enterohepatic circulation, thereby protecting hepatocytes from toxic bile acid accumulation. FXR activation induces distinctive changes in circulating cholesterol in animal models and humans. We present an evaluation of the interaction of various obeticholic acid analogs and other bile salts by studying their binding energies and receptor-ligand interactions using AutoDock software. The results open the possibility of using new alternatives by deriving structures at position 3 of the steroid nucleus.

Academic Editor(s): Name

Published: date

Citation: Seijas, J.A.; Vázquez-Gómez, S.; Meijide, F.; Vázquez-Tato, M.P. In Silico Study of Obeticholic Acid Analogs as FXR Agonists. *Chem. Proc.* **2025**, *volume number*, x. https://doi.org/10.3390/xxxxx

1. Introduction

The farnesoid X receptor (FXR), also known as NR1H4, is a prominent member of the nuclear receptor superfamily [1,2], found mainly in organs such as the liver and gastrointestinal tract. This receptor has been the subject of particular interest due to its pivotal role as a bile acid sensor in enterohepatic tissues. FXR positively regulates cholesterol catabolism and exerts feedback inhibition on bile acid synthesis [3], underlining its importance in maintaining lipid homeostasis. Furthermore, this receptor is suggested to influence the regulation of plasma triglycerides, energy balance, and glucose homeostasis [4]. Given its multifunctionality, FXR is considered a promising potential target for the development of novel pharmacotherapies targeting metabolic diseases, including non-alcoholic fatty liver disease (NAFLD). In recent years, the synthesis and biological evaluation of steroidal FXR agonists have been extensively investigated [5–13]. Modifications were mainly based on the backbone and side chains of chenodeoxy cholic acid (CDCA). Of all the backbone derivatives, obeticholic acid with an ethyl group at the 6-position was found to be the most potent FXR agonist. The 6α-ethyl group may reside in a hydrophobic

cavity within the ligand binding domain of FXR, a key structural element for FXR potency [14].

2. Results and Discussion

In this communication we present a study of the interaction of a group of obeticholic acid derivatives with various functional groups on the crystal structure of the nuclear receptor FXR 1OSV obtained from the RSCB Protein Data Bank [15]. This structure presents obeticholic acid as a ligand and therefore seems ideal for comparing the behavior of the different OCA derivatives. For this purpose, the coordinates of the protein chain A of 1OSV were used and using the Autodock software [16] with MGLTools [17] the different binding energies of compounds **1–42** were calculated (Figure 1) for which the binding energy values indicated in Table 1 were obtained.

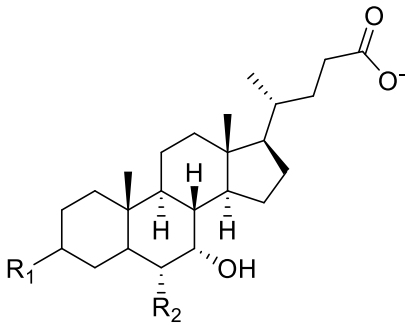

Figure 1. General structure of the OCA derivatives **1–42** studied.

Table 1. Binding energies of compounds **1–42**.

Compound	-R_1	-R_2	kcal/mol
1	β-$HOCH_2CH_2O$-	-Et	−13.41
2	α-SO_3NH_2	-Et	−12.94
3	α-azido	-Et	−12.86
4	=NOH	-Et	−12.79
5	β-t-Bu	-Et	−12.78
6	α-OPO3PO3-	-Et	−12.67
7	β-N_3	-Et	−12.58
8	α-OH (OCA)	-Et	−12.32
9	β-CN	-Et	−12.31
10	α-CN	-Et	−12.1
11	=$NHNH_2$	-Et	−12.08
12	α-NH2	-Et	−12.07
13	α-SH	-Et	−11.99
14	β-SH	-Et	−11.96
15	α-t-Bu	-Et	−11.94
16	β-CH_3	-Et	−11.89
17	β-OPO_3PO_3-	-Et	−11.86
18	β-$NHCSNH_2$	-Et	−11.82
19	β-$NHCONH_2$	-Et	−11.8
20	α-CH_3	-Et	−11.79
21	β-imidazole	-Et	−11.64
22	β-OCH3	-Et	−11.64
23	-H	-Et	−11.53
24	β-OH	-Et	−11.44
25	α-OH (CDC)	-H	−11.30

26	α-OCH_3	-Et	−11.4
27	α-$HOCH_2CH_2O$-	-Et	−11.22
28	β-NH_2	-Et	−11.17
29	α-$NHCSNH_2$	-Et	−11.16
30	α-$NHCONH_2$	-Et	−11.16
31	α-PO_3	-Et	−11.16
32	β-PO_3	-Et	−10.95
33	α-OPO_3	-Et	−10.91
34	α-imidazole	-Et	−10.81
35	β-$NHC(NH)NH_2$	-Et	−10.78
36	β-OPO_3	-Et	−10.5
37	β-CO_2	-Et	−10.42
38	α-CO_2	-Et	−9.61
39	α-$NHC(NH)NH_2$	-Et	−9.52
40	α-SO_3-	-Et	−8
41	β-SO_3-	-Et	−7.96
42	β-SO_3NH_2	-Et	−7.61

Ligands were evaluated using SwissADME [15], to assess pharmacokinetics and small molecule drug-likeness, predictive models of physicochemical properties, pharmacokinetics, drug-likeness and compatibility with medicinal chemistry, including the BOILED-Egg diagram (an intuitive graphical classification model for gastrointestinal absorption and brain access) [16] (Figure 2).

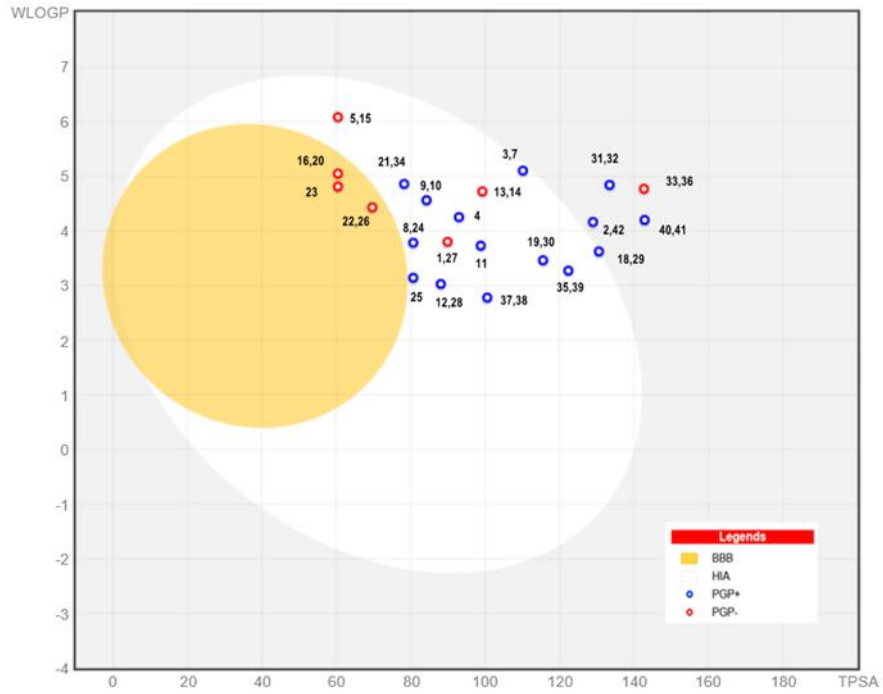

Figure 2. BOILED-Egg diagram for compounds **1–42**.

In Figure 2 the white region is for a high probability of passive absorption by the gastrointestinal tract, the yellow region (yolk) is for a high probability of brain penetration, the blue dots indicate the prediction that they are actively effluent by P-gp (PGP+) and the red ones if it is predicted that they will not be effluxed from the central nervous system by P-glycoprotein P-gp (PGP−). Other results obtained are listed in Table 2. These include the number of acceptor and donor atoms in hydrogen bonds in each ligand

molecule, the topological polar surface area (TSPA), the mean LogP, the gastrointestinal absorption (GIA), the permeation across the blood-brain barrier (BBB), the consensus LogP by various methods, transport by P-glycoprotein (PGP), Knowledge about whether the compounds are substrate or non-substrate of the permeability glycoprotein is key to assess the active efflux through biological membranes, for example, from the gastrointestinal wall to the lumen or from the brain. An important function of P-gp is to protect the central nervous system (CNS) from xenobiotics [15] and the prediction about its ability to inhibit cytochromes P-450: 1 A2, 2C19, 2C9, 2D6 and 3 A4, the inhibition of these isoenzymes is undoubtedly one of the main causes of pharmacokinetic interactions between drugs, which cause toxic adverse effects or other unwanted adverse effects due to the lower clearance and accumulation of the drug or its metabolites [15].

Table 2. SwissADME predictions for compounds **1–41**. Ha: hydrogen bond acceptor, Hd: hydrogen bond donor, TPSA: topological polar surface area (Å^2), LogP: consensus Log$P_{o/w}$, GIA: gastrointestinal absorption according to boiled egg diagram, BBBP: brain blood barrier permeation, PGP: P-glycoprotein substrate, CYP: cytochrome P450 inhibitor.

Cpd	Ha	Hb	TPSA	LOG	GIA	BBB	PGP	CYP1A2	CYP1A2	CYP2C19	CYP2C9	CYP2D6
1.27	5	2	89.82	3.89	High	No	No	No	No	No	No	Yes
2.42	6	2	128.9	3.14	Low	No	Yes	No	No	No	No	No
3.7	6	1	110.11	4.35	High	No	Yes	No	No	No	No	No
4	5	2	92.95	4.31	High	No	Yes	No	No	Yes	No	No
5.15	3	1	60.36	6.28	High	No	No	No	No	No	No	No
6.17	10	1	201.76	2.51	Low	No	No	No	No	No	No	Yes
8.24	4	2	80.59	3.90	High	No	Yes	No	No	No	No	No
9.10	4	1	84.15	4.64	High	No	Yes	No	No	Yes	No	No
11	4	2	98.74	4.09	High	No	Yes	No	No	No	No	No
12.28	3	2	88	2.44	High	No	Yes	No	No	No	No	No
13.14	3	1	99.16	4.63	High	No	No	No	Yes	No	No	No
16.20	3	1	60.36	5.03	High	Yes	No	No	No	No	No	No
18.29	3	3	130.5	3.88	Low	No	Yes	No	Yes	No	No	Yes
19.30	4	3	115.48	3.35	High	No	Yes	No	No	No	No	Yes
21.34	4	1	78.18	4.19	High	No	Yes	No	No	No	No	No
23	3	1	60.36	4.80	High	Yes	No	No	No	No	No	No
25	4	2	80.59	3.35	High	No	Yes	No	No	No	No	No
22.26	4	1	69.59	4.32	High	Yes	No	No	No	No	No	No
31.32	6	1	133.36	3.28	Low	No	Yes	No	Yes	No	No	No
33.36	7	1	142.59	3.25	Low	No	No	No	Yes	No	No	No
35.39	4	4	122.26	3.32	High	No	Yes	No	No	No	No	Yes
37.38	5	1	100.49	3.72	High	No	Yes	No	No	No	No	Yes
40.41	6	1	142.76	3.05	Low	No	Yes	No	Yes	No	No	No

For each of the ligands, the complex that the Autodock program indicated with a more favorable binding energy, that is, more negative, was chosen. As a reference, the 1OSV crystal structure was analyzed, and the ligand-receptor interactions were extracted using the Discovery Studio Visualizer program [17] to identify the residues that interact with the ligand.

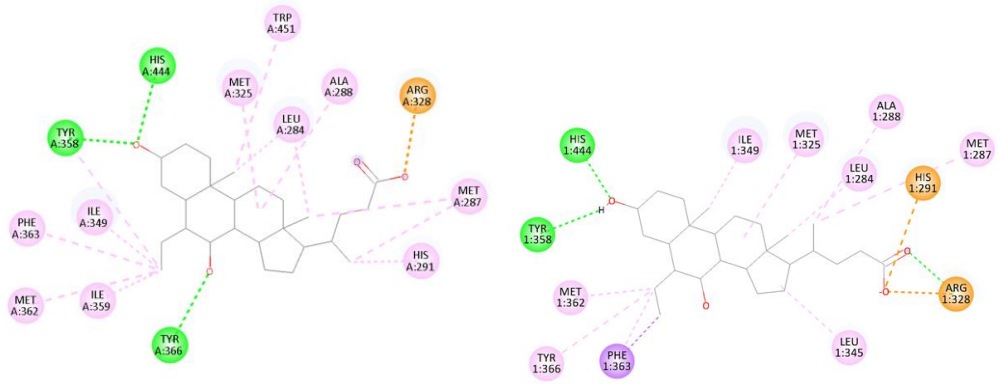

Figure 3. Interactions ligand-receptor for 1OSV (left) and complex (**8**) with obeticholic calculated with Autodock.

The noncovalent interaction (NCI) method, also known as the reduced density gradient (RDG) method, is very popular for studying weak interactions [18]. These interactions are crucial for determining how a ligand, such as a drug or a substrate in a chemical reaction, binds to a target molecule, such as a protein or a catalyst. Calculating the reduced density gradient (RDG) using the promolecular approach is a reasonably reliable alternative for working with macromolecules, where the binding mode of proteins and ligands is studied; it avoids the high time and resource costs of ab initio calculations. The promolecular density is constructed by simply superimposing the electron densities of the free atoms and can therefore be easily evaluated. RDG and NCI surfaces were calculated with software Multiwfn [19,20].

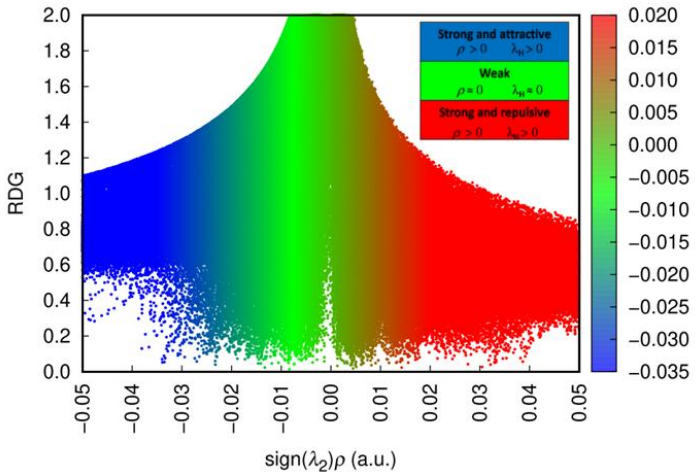

Figure 4. Scatter map of RDG and sign(λ_2)ϱ.

The energy binding calculated for obeticholic acid is −12.32 kcal/mol. Complexes **1–7** present more favorable binding energies, the interaction with near residues to 3-C substituent is with TYR358 remains in **1,2,4** HIS444 in **3,6,7** and HIS444, MET447 and TRP451 for **5**.

In complex **9** the β-cyano group in 3C has no interaction with resides but the epimer **10** with the α-cyano group interacts with HIS444. In complex **11** hydrazone interacts with TYR358, as does complex **12** which is under zwitterionic form, but this also shows an unfavorable positive-positive interaction with HIS444.

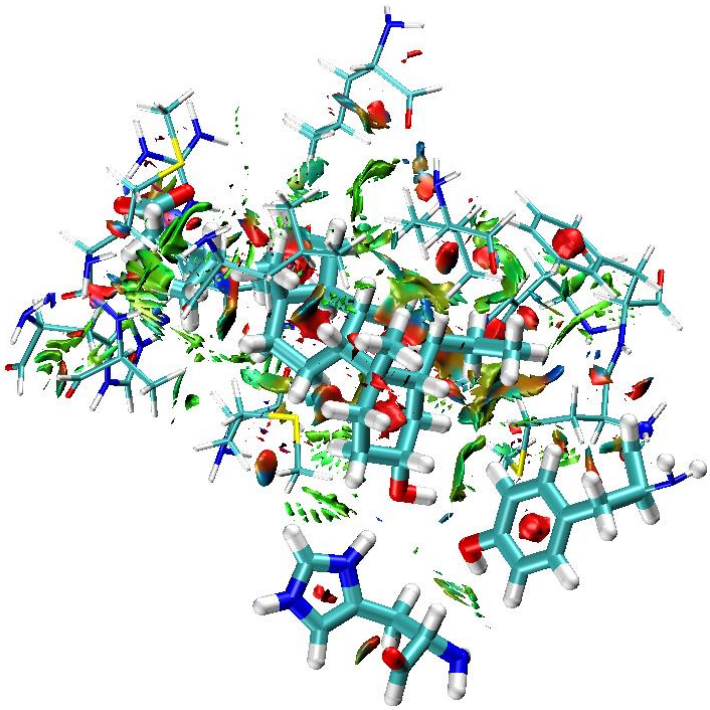

Figure 5. NCI surface for **8**, TYR358 and HIS444 in thick bonds.

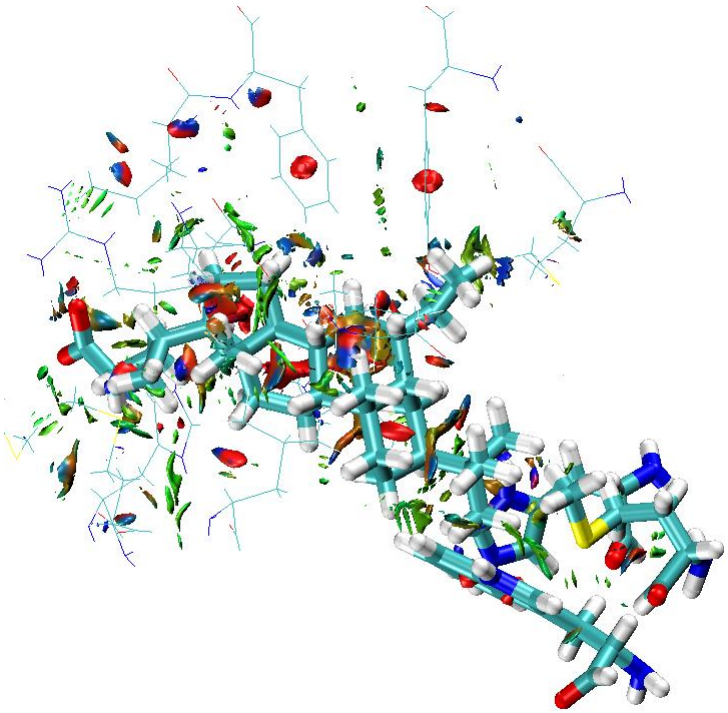

Figure 5. NCI surface for **5**, interactions with HIS444, MET447 and TRP451.

Thiol complexes **13** and **14** show both interaction by hydrogen bonding with TYR358, but 14 shows and additional pi-sulfur interactions with HIS444.

Chenodeoxycholic acid (CDC, **25**) lacks the ethyl substituent at 7-C present in obeticholic acid (OCA, **8**). Interactions with nearest residues are similar only the ethyl substituent interactions are absent as expected (Figures 7 and 8).

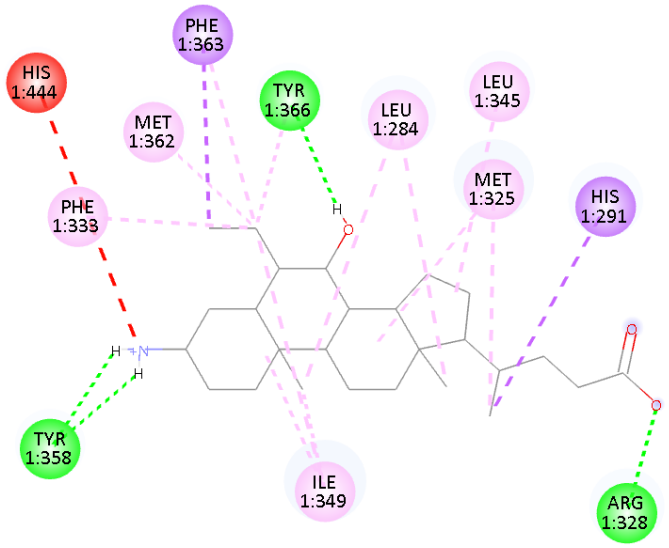

Figure 6. Interactions of ligand **12** with near residues.

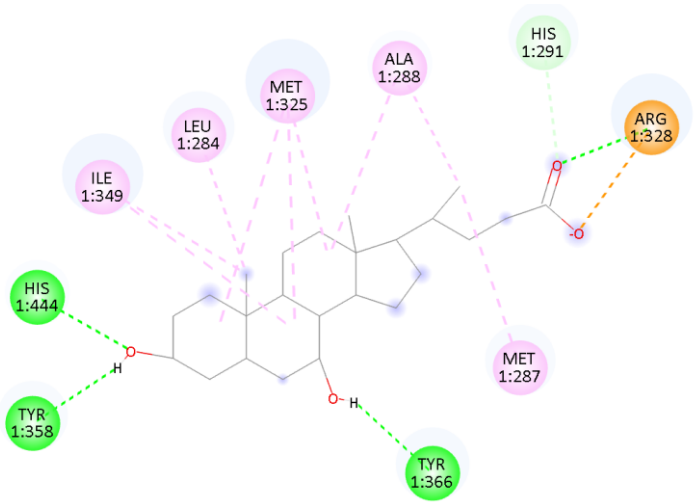

Figure 7. Interactions in complex **25**.

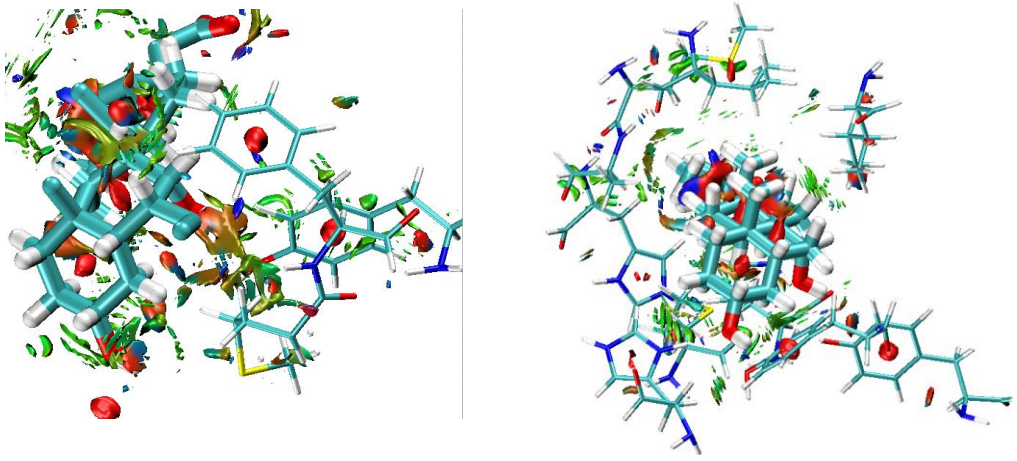

(**a**) (**b**)

Figure 8. NCI surfaces plot for **8** (**a**) and **25** (**b**).

In Figure 8b it can be observed that there are no interactions between 7-C and residues in the peptide. When complex **23** was calculated the interactions with MET362, PHE363 and TYR366 present in **8** are maintained even with the absence of hydroxyl group in 3-C (Figure 9).

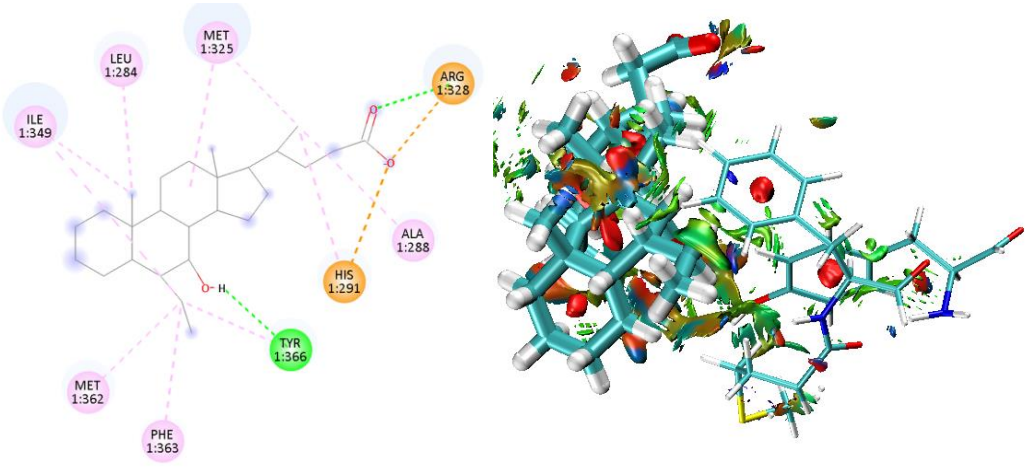

(**a**) (**b**)

Figure 9. Interactions of compound 23 (**a**) and NCI surfaces (**b**).

Compounds **2**, **18**, **33**, **31**, **32**, **36**, **40**, **41** and **42** are out of scale in the BOILED-Egg diagram, so in principle they would be discarded despite the favorable binding energy of **2.** If we consider the binding energy of chenodeoxycholic acid as a lower limit, the compounds that would penetrate the BBB would be **16** (β-CH3), **20** (α-CH3), **22** (β-OCH3), **23** (-H) and **26** (α-OCH3) could be interesting options. The rest of the compounds present acceptable gastrointestinal absorption and PGP and CYP inhibition.

3. Conclusions

After having studied 41 variants for the substitution at carbon 3 of the skeleton of obeticholic acid (**8**) and chenodeoxycholic acid (**25**), it has been found that compounds **1**–**7** have better binding energies than 8. Of these seven compounds, only **2** is not expected to present a good gastrointestinal absorption, so that compounds with the following functional groups at carbon 3: β-HOCH2CH2O-, α-SO3NH2,α-N3, =NOH,β-tBu,α-OPO3PO3-,β N3 would be candidates with potential biological activity for in vitro tests.

Author Contributions: J.A.S. and M.P.V.-T.: Conceptualization and methodology; J.A.S., M.P.V.-T., S.V.-G. and F.M.: formal analysis, investigation and writing—original draft preparation, JASV writing—review and editing. All authors have read and agreed to the published version of the manuscript.

Acknowledgments: Galicia Supercomputing centrer (CESGA) for providing computing facilities.

References

1. Forman, B.M.; Goode, E.; Chen, J.; Oro, A.E.; Bradley, D.J.; Perlmann, T.; Noonan, D.J.; Burka, L.T.; McMorris, T.; Lamph, W.W.; et al. Identification of a nuclear receptor that is activated by farnesol metabolites. *Cell* **1995**, *81*, 687–693. https://doi.org/10.1016/0092-8674(95)90530-8.
2. Seol, W.; Choi, H.S.; Moore, D.D. Isolation of proteins that interact specifically with the retinoid X receptor: Two novel orphan receptors. *Mol. Endocrinol.* **1995**, *9*, 72–85. https://doi.org/10.1210/mend.9.1.7760852.
3. Chen, W.; Owsley, E. Nuclear receptor-mediated repression of human cholesterol 7-α-hydroxylase gene transcription by bile acids *J. Lipid Res.* **2001**, *42*, 1402–1412. https://doi.org/10.1016/S0022-2275(20)30272-8.
4. Jiao, Y.; Lu, Y.; Li, X. Farnesoid X receptor: A master regulator of hepatic Triglyceride and glucose homeostasis. *Acta Pharmacol. Sin*. **2015**, *36*, 44–50. https://doi.org/10.1038/aps.2014.116.
5. Iguchi, Y.; Kihira, K.; Nishimaki-Mogami, T.; Une, M. Structure–activity relationship of bile alcohols as human farnesoid X receptor agonist. *Steroids* **2010**, *75*, 95–100. https://doi.org/10.1016/j.steroids.2009.11.002.
6. Pellicciari, R.; Gioiello, A.; Costantino, G.; Sadeghpour, B.M.; Rizzo, G.; Meyer, U.; Parks, D.J.; Entrena-Guadix, A.; Fiorucci, S. Back door modulation of the farnesoid X receptor: Design, synthesis, and biological evaluation of a series of side chain modified chenodeoxycholic acid derivatives. *J. Med. Chem.* **2006**, *49*, 4208–4215. https://doi.org/10.1021/jm060294k.
7. Fujino, T.; Mizuho, U.; Imanaka, T. Structure-activity relationship of bile acids and bile acid analogs in regard to FXR activation. *J. Lipid Res*. **2004**, *45*, 132–138. https://doi.org/10.1194/jlr.M300215-JLR200.
8. Gioiello, A.; Macchiarulo, A. Extending SAR of bile acids as FXR ligands: Discovery of 23-N-(carbocinnamyloxy)-3α,7α-dihydroxy-6α ethyl-24-nor-5β-cholan-23-amine. *Bioorg. Med. Chem.* **2011**, *19*, 2650–2658. https://doi.org/10.1016/j.bmc.2011.03.004.
9. Pellicciari, R.; Costantino, G. Bile Acid Derivatives as Ligands of the Farnesoid X Receptor. Synthesis, Evaluation, and Structure−Activity Relationship of a Series of Body and Side Chain Modified Analogues of Chenodeoxycholic Acid. *J. Med. Chem.* **2004**, *47*, 4559–4569. https://doi.org/10.1021/jm049904b.
10. Pellicciari, R.; Costantino, G. Farnesoid X Receptor: From Structure to Potential Clinical Applications. *J. Med. Chem*. **2005**, *48*, 5383–5403. https://doi.org/10.1021/jm0582221.
11. Mi, L.Z.; Devarakonda, S. Structural basis for bile acid binding and activation of the nuclear receptor FXR. *Mol. Cell* **2003**, *11*, 1093–1100. https://doi.org/10.1016/s1097-2765(03)00112-6.
12. Merk, D.; Steinhilber, D.; Schubert-Zsilavecz, M. Medicinal chemistry of farnesoid X receptor ligands: From agonists and antagonists to modulators. *Future Med. Chem.* **2012**, *4*, 1015–1036. https://doi.org/10.4155/fmc.12.47.
13. Coleman, J.P.; Kirby, L.C. Metabolic fate and hepatocyte toxicity of reverse amide analogs of conjugated ursodeoxycholate in the rat. *J. Steroid Biochem. Mol. Biol.* **1998**, *64*, 91–101. https://doi.org/10.1016/s0960-0760(97)00138-6.
14. Pellicciari, R.; Fiorucci, S.; Camaioni, E.; Clerici, C.; Costantino, G.; Maloney, P.R.; Morelli, A.; Parks, D.J.; Willson, T.M. 6-Ethyl-chenodeoxycholic acid (6- ECDCA), a potent and selective FXR agonist endowed with anticholestatic activity. *J. Med. Chem*. **2002**, *45*, 3569–3572. https://doi.org/10.1021/jm025529g.
15. Daina, A.; Michielin, O.; Zoete, V. SwissADME: A free web tool to evaluate pharmacokinetics, drug-likeness and medicinal chemistry friendliness of small molecules. *Sci. Rep*. **2017**, *7*, 42717. https://doi.org/10.1038/srep42717.
16. Daina, A.; Zoete, V A BOILED-Egg to predict gastrointestinal absorption and brain penetration of small molecules. *ChemMedChem* **2016**, *11*, 1117–1121. https://doi.org/10.1002/cmdc.201600182.
17. Discovery Studio Visualizer v25.1.02484. ©2025 Dassault Systèmes Biovia Corp.
18. Johnson, E.R.; Keinan, S.; Mori-Sánchez, P.; Contreras-García, J.; Cohen, A.J.; Yang, W. Revealing Nocovalent Interactions. *J. Am. Chem. Soc*. **2010**, *132*, 6498–6506.
19. Lu, T.; Chen, F. Multiwfn: A multifunctional wavefunction analyzer. *J. Comput. Chem.* **2012**, *33*, 580–592. https://doi.org/10.1002/jcc.22885.
20. Lu, T. A comprehensive electron wavefunction analysis toolbox for chemists, Multiwfn. *J. Chem. Phys.* **2024**, *161*, 082503. https://doi.org/10.1063/5.0216272.